

Calculated Spin Fluctuational Pairing Interaction in $\text{HgBa}_2\text{CuO}_4$ using LDA+FLEX Method

Griffin Heier and Sergey Y. Savrasov

Department of Physics, University of California, Davis, CA 95616, USA

(Dated: January 30, 2024)

A combination of density functional theory in its local density approximation (LDA) with \mathbf{k} - and ω dependent self-energy found from fluctuational-exchange-type random phase approximation (FLEX-RPA) is utilized here to study superconducting pairing interaction in a prototype cuprate superconductor $\text{HgBa}_2\text{CuO}_4$. Although, FLEX-RPA methodology have been widely applied in the past to unconventional superconductors, previous studies were mostly based on tight-binding derived minimal Hamiltonians, while the approach presented here deals directly with the first principle electronic structure calculation of the studied material where spin and charge susceptibilities are evaluated for a correlated subset of the electronic Hilbert space as it is done in popular LDA+U and LDA+DMFT methods. Based on our numerically extracted pairing interaction among the Fermi surface electrons we exactly diagonalize a linearized BCS gap equation, whose highest eigenstate is expectantly found corresponding to $d_{x^2-y^2}$ symmetry for a wide range of on-site Coulomb repulsions U and dopings that we treat using virtual crystal approximation. Calculated normal state self-energies show a weak \mathbf{k} - and strong frequency dependence with particularly large electronic mass enhancement in the vicinity of spin density wave instability. Although the results presented here do not bring any surprisingly new physics to this very old problem, our approach is an attempt to establish the numerical procedure to evaluate material specific coupling constant λ for high T_c superconductors without reliance on tight-binding approximations of their electronic structures.

PACS numbers:

I. INTRODUCTION.

Shortly before the discovery of high-temperature superconductivity in cuprates in 1986[1], two seminal works [2, 3] have been published in an attempt to understand properties of heavy fermion superconductors by the pairing of their Fermi surface electrons mediated by strong (anti)ferromagnetic spin fluctuations which can lead to symmetries of the superconducting state of angular momenta higher than zero. Although such random-phase approximation (RPA) based calculations deemed oversimplified, the divergency of spin susceptibility in the vicinity of the magnetic, spin density wave (SDW) type instability due to the Fermi surface nesting is a common feature of many unconventional superconductors which this method naturally incorporates. The approach took off right after doped La_2CuO_4 was shown to superconduct at 33K[4] and has been applied since then to study unconventional superconductivity phenomenon [5] in a great variety of materials, such as cuprates[6–9], ruthenates[10, 11], cobaltates[12], ironates [13–16], heavy fermion[17, 18] systems, and most recently, nickelates[19, 20].

To date, most of these applications however utilize simple few-orbital models where the hopping integrals are extracted from density functional based calculations using such popular approximations as Local Density Approximation (LDA)[21], and these parameters are subsequently treated as the input to the Hubbard-type model Hamiltonians. The latter is then solved by an available many-body technique, such, for example, as the Fluc-

tuational Exchange Approximation (FLEX) [22]. FLEX is a diagrammatic approach that includes particle-hole ladders and bubbles as well as particle-particle ladder diagrams while the RPA neglects the latter contribution. However, it was found to be sufficiently small [23] at least for the problem of paramagnons[24, 25] where the most divergent terms are given by the particle-hole ladders.

Many past studies of strongly correlated systems have been performed using the RPA and FLEX [26] including the proposals to combine it with density functional electronic structure calculations [27]. More recently developed combination of LDA with Dynamical Mean Field Theory (LDA+DMFT)[28] sometimes utilizes the local FLEX approximation to solve corresponding impurity problem during the self-consistent solution of the DMFT equations. A further combination of FLEX and DMFT was also proposed recently and has resulted in reproducing a doping dependence of critical temperature seen in cuprates [29]. More rigorous Quantum Monte Carlo based simulations provide further extensions to this approach[30, 31].

We have recently described an implementation of the LDA+FLEX(RPA)[32] approach using the method of projectors which allows to evaluate dynamical susceptibilities of the electrons in a Hilbert space restricted by correlated orbitals only. This is very similar to how it is done in such popular electronic structure techniques as LDA+U[33, 34] and LDA+DMFT[28]. The projector formalism tremendously simplifies the numerics and allows to incorporate \mathbf{k} - and ω dependent self-energies of correlated electrons straight into the LDA electronic

structure calculation. Our applications to V and Pd [32] have, in particular, showed that the d–electron self–energies in these materials are remarkably k –independent which justifies the use of local self–energy approximations, such as DMFT.

Here, we extend the projector based LDA+FLEX approach to evaluate superconducting pairing interactions describing the scattering of the Cooper pairs at the Fermi surface in a realistic material framework. We utilize density functional calculation of the electronic energy bands and wave functions for $\text{HgBa}_2\text{CuO}_4$, a prototype single–layer cuprate whose superconducting T_c was reported to be 94K[35]. Based on our numerically evaluated pairing function we exactly diagonalize a linearized BCS gap equation on a three dimensional k –grid of points in the Brillouin Zone. The extracted highest (in value) eigenstate from this procedure is unsurprisingly found to correspond to $d_{x^2-y^2}$ symmetry for a wide range of on–site Coulomb repulsions U and dopings that we scan during our simulations. The corresponding maximum eigenvalue λ_{max} represents a coupling constant similar to the parameter λ_{e-p} of the electron–phonon (e-p) theory of superconductivity. Our primary goal here is to establish a numerical procedure for the material specific evaluation of this coupling constant that can hopefully be helpful in future findings of the materials with high T_c . We however found λ_{max} to be very sensitive to the values of U used in our calculation once we approach the region of antiferromagnetic instability. The same is seen in our calculated normal state self–energies which were found to show a weak \mathbf{k} – and strong frequency dependence with particularly large electronic mass renormalization $m^*/m_{LDA} = 1 + \lambda_{sf}$ in the proximity to SDW. The evaluated renormalized coupling constant $\lambda_{eff} = \lambda_{\text{max}} / (1 + \lambda_{sf})$ is found to be modest and incapable to deliver the high T_c values unless we tune U to be close to SDW. Using the available experimental constraints on the values of $\lambda_{sf} \lesssim 3$, we find $\lambda_{eff} \lesssim 0.4$ and the BCS $T_c \lesssim 30K$. Despite it looks like an underestimation, we think the approach opens up better opportunities to find material specific dependence of the T_c in unconventional superconductors without reliance on tight–binding approximations of their electronic structures.

Our paper is organized as follows: In Section II we summarize the approach to evaluate the pairing interaction using the LDA+FLEX formalism. In Section III we discuss our results of exact diagonalization of the linearized BCS equation and correspondingly extracted superconducting energy gaps and the eigenvalues as a function of U and doping. We also present our results for correlated electronic structure in $\text{HgBa}_2\text{CuO}_4$ in the normal state, the calculated mass enhancement, the effective coupling constant λ_{eff} and finally give some estimates for the T_c . Section V is the conclusion.

II. METHOD

a. Superconducting Pairing Interaction from LDA+FLEX.

Our assumption here is that a general spin–dependent interaction is operating between the electrons at the Fermi surface

$$K^{\nu_1\nu_2\nu_3\nu_4}(\mathbf{r}_1, \mathbf{r}_2, \mathbf{r}_3, \mathbf{r}_4). \quad (1)$$

Here for the sake of numerical simplicity we make one important approximation to consider this interaction as static and operating between the electrons only in the close proximity to the Fermi energy exactly as the BCS theory assumes. The inclusion of its frequency dependence is of course possible and has been done previously in many model calculations but we postpone such implementation for real materials for the future.

For the non–relativistic formulation that is adopted here, due to full rotational invariance of the spin space, the actual dependence of this interaction on spin indexes appears to be the following

$$K^{\nu_1\nu_2\nu_3\nu_4} = \frac{1}{2}\delta_{\nu_1\nu_3}\delta_{\nu_2\nu_4}K^c - \frac{1}{2}\sigma_{\nu_1\nu_3}\sigma_{\nu_2\nu_4}K^s,$$

where the interactions K^c and K^s are due to charge and spin degrees of freedom, and σ are the Pauli matrices. Transformation to singlet–triplet representation is performed using the eigenvectors $A_{\nu_1\nu_2}^{SS_z}$ of the product for two spin operators which leads us to consider the interactions for the singlet ($S = 0, S_z = 0$) and triplet ($S = 1, S_z = -1, 0, +1$) states separately

$$\begin{aligned} K^{(S'S'_zSS_z)} &= \sum_{\nu_1\nu_2\nu_3\nu_4} A_{\nu_1\nu_2}^{S'S'_z} K^{\nu_1\nu_2\nu_3\nu_4} A_{\nu_3\nu_4}^{SS_z} \\ &= \delta_{S'S'}\delta_{S'_zS_z} K^{(S)}, \end{aligned}$$

where $K^{(S)} = \frac{1}{2}K^c - \frac{1}{2}E_S K^s$, and $E_{S=0} = -3, E_{S=1} = +1$ are the eigenvalues for the spin product operators.

We next introduce the matrix elements of scattering between the Cooper pair wave functions $\Psi_{\mathbf{k}j,SS_z}^{(\nu_1\nu_2)}(\mathbf{r}_1, \mathbf{r}_2)$ which are proper antisymmetric combinations of the electronic wave functions with their Fermi momenta \mathbf{k} and $-\mathbf{k}$ in a given energy band labeled by index j . In the singlet–triplet representation these matrix elements are diagonal with respect to the spin indexes and do not depend on S_z

$$\sum_{\nu_1\nu_2\nu_3\nu_4} \langle \Psi_{\mathbf{k}j,SS_z}^{(\nu_1\nu_2)} | K^{\nu_1\nu_2\nu_3\nu_4} | \Psi_{\mathbf{k}'j',S'S'_z}^{(\nu_3\nu_4)} \rangle = \delta_{S'S'}\delta_{S'_zS_z} M_{\mathbf{k}j\mathbf{k}'j'}^{(S)}. \quad (2)$$

Since one–electron wave functions forming the Cooper pairs should obey the Bloch theorem, the integration in the matrix elements can be reduced to the integration

over a single unit cell which leads us to consider the pairing interaction in terms of its lattice Fourier transforms with various combinations of $\pm\mathbf{k}$ and $\pm\mathbf{k}'$ of the type:

$$K_{\mathbf{k},\mathbf{k}'}^{(S)}(\mathbf{r}_1, \mathbf{r}_2, \mathbf{r}_3, \mathbf{r}_4) = \sum_{R_1 R_2 R_3 R_4} e^{-i\mathbf{k}(\mathbf{R}_1 - \mathbf{R}_2)} e^{i\mathbf{k}'(\mathbf{R}_3 - \mathbf{R}_4)} \times K^{(S)}(\mathbf{r}_1 - \mathbf{R}_1, \mathbf{r}_2 - \mathbf{R}_2, \mathbf{r}_3 - \mathbf{R}_3, \mathbf{r}_4 - \mathbf{R}_4).$$

(Due to translational periodicity one lattice sum should be omitted.)

The Cooper pair wave functions can be constructed from corresponding single-electron states that are easily accessible in any density functional based electronic structure calculation. However, the formidable theoretical problem is to evaluate the pairing interaction $K^{(S)}$. Our first approximation to this function is to assume that it operates for correlated subset of electrons which are introduced with help of site dependent projector operators: $\phi_a(\mathbf{r}) = \phi_l(r) i^l Y_{lm}(\hat{r})$ of the one-electron Schroedinger equation taken with a spherically symmetric part of the full potential. [36]. The Hilbert space $\{a\}$ inside the designated correlated site restricts the full orbital set by a subset of correlated orbitals, such as those corresponding to $l = 2$ for Cu. We therefore write

$$K_{\mathbf{k},\mathbf{k}'}^{(S)}(\mathbf{r}_1, \mathbf{r}_2, \mathbf{r}_3, \mathbf{r}_4) = \sum_{a_1 a_2 a_3 a_4} \phi_{a_1}(\mathbf{r}_1) \phi_{a_2}(\mathbf{r}_2) K_{a_1 a_2 a_3 a_4}^{(S)}(\mathbf{k}, \mathbf{k}') \phi_{a_3}^*(\mathbf{r}_3) \phi_{a_4}^*(\mathbf{r}_4)$$

Our second approximation is to adopt the LDA+FLEX(RPA) procedure for evaluating the matrix $K_{a_1 a_2 a_3 a_4}^{(S)}(\mathbf{k}, \mathbf{k}')$ (static for this particular problem, but ω dependent in general). Namely, we represent it in terms of screening the on-site Coulomb interaction matrix $I_{a_1 a_2 a_3 a_4}$ (we drop all indexes hereafter as this becomes just the matrix manipulation)

$$\hat{K} = \hat{I} + \hat{I}[\hat{\chi} - \frac{1}{2}\hat{\pi}]\hat{I}.$$

Here the interacting susceptibility $\hat{\chi} = \hat{\pi}[\hat{1} - \hat{I}\hat{\pi}]^{-1}$, $\hat{\pi}$ is the non-interacting polarizability, and the subtraction of $\frac{1}{2}\hat{\pi}$ takes care of the single bubble diagram that appears twice in both bubble and ladder series. Remind that the matrix \hat{I} is local in space since it describes the on-site Coulomb repulsion U . Due to this notion of locality, the screened matrix $K_{a_1 a_2 a_3 a_4}^{(S)}(\mathbf{k}, \mathbf{k}')$ becomes dependent only on $\mathbf{k} \pm \mathbf{k}'$.

The procedure to calculate the matrix \hat{K} using density functional based electronic structure for real materials was described in details in our previous publication [32]. Here we would only like to point out that it is still a computationally demanding problem since the matrices need to be computed for dense set of wavevectors and their frequency dependence is also generally required. The restriction by the correlated subset tremendously

simplifies all matrix manipulations with the ladder diagrams that rely on the 4-point functions scaling with the number of atoms in the unit cell as N_{atom}^4 . This is contrary to the bubble diagrams which rely on the two-point functions scaling as N_{atom}^2 , and are in the heart of such popular method as GW[37]. However, the use of the on-site interaction in ladder diagrams allows one to express all quantities via charge and spin susceptibilities which are the two-point functions and allow to regain the N_{atom}^2 scaling. It is still computationally involved because the number of matrix elements for representing the susceptibility grows as $N_{atom}^2 N_{orb}^4$ where N_{orb} is the size of complete orbital manifold per atom needed. For HgBa₂CuO₄, $N_{atom} = 8$, $N_{orb} = 9$ for Hg, Ba, Cu ($l_{max} \leq 2$) and $N_{orb} = 4$ for O ($l_{max} \leq 1$), this requires at least $4^2 \times 9^4 + 4^2 \times 4^4 = 109,072$ matrix elements to be computed for each wave vector and frequency! Often, to improve the accuracy, the number of orbitals per each angular harmonic needs to be doubled or tripled which blows up the matrices by another one to two orders due to N^4 scaling. The restriction by the correlated subset greatly facilitates the calculation, because now the matrices have to be computed for the correlated sites and orbitals only, and for the problem at hand, 5 orbital states representing Cu d-electrons produce only $1^2 \times 5^4 = 625$ matrix elements.

b. Spin Fluctuational Coupling Constant

The matrix elements $M_{\mathbf{k}j\mathbf{k}'j'}^{(S)}$ which scatter the Cooper pairs enter the Eliashberg gap equation for superconducting T_c . Numerous solutions of this equation have been implemented in the past for the single- and multi-orbital Hubbard models to address the question of unconventional superconductivity in cuprates and other systems [6, 8, 9, 11, 13]. These implementations involve both the FLEX and more sophisticated Dynamical Cluster Approximation (DCA)[30, 31] for the pairing interaction; they work on the imaginary Matsubara frequency axis and do not determine the coupling constant directly, but go straight to the T_c . The self-consistency is important as it allows to account for many effects known from the theory of superconductivity. In particular, the mass of the quasiparticles is known to renormalize due to the attractive pairing interaction operating at some small energy scale, set, *e.g.*, by a spin fluctuational energy ω_{sf} . Also, the Coulomb repulsion that operates at much larger energy scale, such as plasmon energy ω_p , weakens the coupling of the Cooper pairs somewhat.

Establishing numerical procedure for estimating the coupling constant for unconventional superconductors is central for understanding material specific trends of their critical temperatures. This was earlier the case for electron-phonon (e-p) superconductors [38], where, in most cases, the solution of the gap equation is given by the momentum independent gap function in the sin-

glet pairing channel, that corresponds to λ_{e-p} . Luckily, phonons have a well-defined cutoff frequency which is the phonon Debye energy ω_D , and the equation for T_c is often treated in the BCS approximation, i.e., when the pairing between the electrons resides only in a small energy window $\pm\omega_D$ around the Fermi energy ϵ_F , and where the matrix elements $M_{\mathbf{k}j\mathbf{k}'j'}^{(S)}$ are assumed to be constant, and zero outside those energies. The quasiparticle mass enhancement, $m^*/m = 1 + \lambda_{e-p}$, that leads to a kink in the single-particle spectrum at the scale ω_D and the effects of the Coulomb interaction that weaken the coupling constant λ_{e-p} by the parameter μ^* (usually very small, ~ 0.1 , due to different energy scales ω_D vs. ω_p [39]) are taken into account by utilizing the renormalized coupling constant $\lambda_{eff} = (\lambda_{e-p} - \mu^*)/(1 + \lambda_{e-p})$ that determines the T_c . With a few empirically adjusted coefficients this gave rise to the famous McMillan T_c equation [40]. One, in principle, does not need this simplified point of view and can proceed with the Eliashberg equation, but in a semiquantitative way, the McMillan theory is known to work very well.

In the following we adopt the BCS approximation by assuming that the pairing occurs in a small region around the Fermi surface restricted by some spin fluctuational frequency ω_{sf} . Although for a generally screened electron-electron interaction there is no formal justification to separate such small energy scale, it is known that spin fluctuations have a characteristic energy ω_{sf} similar to phonons, and that experimentally, in cuprates they have been seen in the range of energies 30–50 meV as peaks in imaginary spin susceptibility accessible via the numerous neutron scattering experiments [41]. There is a famous 40 meV resonance which is visible in the superconducting state [42]. There are numerous angle resolved photoemission experiments (ARPES) that show kinks in the one-electron spectra at the same energy range [43]. These kinks are sometimes interpreted as caused by the electron-phonon interactions [44], but, unfortunately, the calculated values of λ_{e-p} are known to be small in the cuprates [45, 46]. Note also that for the undoped antiferromagnetic cuprates, the spin wave spectra reside in the energy range of 30 meV [47].

Thus, we will assume that the matrix elements $M_{\mathbf{k}j\mathbf{k}'j'}^{(S)}$ which scatter the Cooper pairs enter the linearized BCS equation

$$\Delta_S(\mathbf{k}j) = -\frac{1}{2} \sum_{\mathbf{k}'j' \in \epsilon_F \pm \omega_{sf}} M_{\mathbf{k}j\mathbf{k}'j'}^{(S)} \Delta_S(\mathbf{k}'j') \times \tanh\left(\frac{\epsilon_{\mathbf{k}'j'}}{2T_c}\right) / 2\epsilon_{\mathbf{k}'j'}. \quad (3)$$

where the summation over $\mathbf{k}'j'$ goes over the electrons residing in a small region around the Fermi surface restricted by ω_{sf} . The solutions $\Delta_S(\mathbf{k}j)$ for $S = 0$ or 1 describe momentum dependence of superconducting en-

ergy gap and are known to be either even or odd functions of momenta. Performing the integration over the energy window $\epsilon_F \pm \omega_{sf}$ we rewrite the equation in a form

$$-\ln\left(\frac{1.134\omega_{sf}}{T_c}\right) \sum_{i'} M^{(S)}(\hat{k}_i, \hat{k}_{i'}) \frac{\delta A_{i'}}{|v_{i'}|} \Delta_S(\hat{k}_{i'}) = \Delta_S(\hat{k}_i),$$

Here we introduced some discretization of the Fermi surface onto small areas δA_i with absolute values of the electronic velocities $|v_i|$ whose locations are pointed by the Fermi momenta \hat{k}_i . To view this expression as diagonalization in ii' indexes, we treat $\Delta_S(\hat{k}_i)$ as eigenvectors and multiply the right hand part by a set of eigenvalues $\varepsilon^{(\kappa)}$ bearing in mind that the physical solution for $\Delta_S^{(\kappa)}(\hat{k}_i)$ is given when the highest eigenvalue $\varepsilon^{(\kappa)}$ becomes unity. We thus obtain the Hermitian eigenvalue problem

$$\sum_{i'} \left[\sqrt{\frac{\delta A_i}{|v_i|}} M^{(S)}(\hat{k}_i, \hat{k}_{i'}) \sqrt{\frac{\delta A_{i'}}{|v_{i'}|}} - \delta_{ii'} \frac{\varepsilon^{(\kappa)}}{\ln\left(\frac{1.134\omega_{sf}}{T_c}\right)} \right] \times \sqrt{\frac{\delta A_{i'}}{|v_{i'}|}} \Delta_S^{(\kappa)}(\hat{k}_{i'}) = 0, \quad (4)$$

where the renormalized eigenvalues $\lambda^{(\kappa)} = \varepsilon^{(\kappa)} / \ln\left(\frac{1.134\omega_{sf}}{T_c}\right)$ come out as a result of diagonalization. The condition $\varepsilon^{(\kappa)} = 1$ for some $\kappa = m$ means that the highest renormalized eigenvalue $\lambda^{(m)} = \max\{\lambda^{(\kappa)}\} \equiv \lambda_{\max}$ is the physical one which delivers $\Delta_S^{(m)}(\hat{k}_i)$ and produces the famous BCS equation for $T_c = 1.134\omega_{sf} \exp(-1/\lambda_{\max})$.

We further modify the coupling constant that enters this equation to take into account the discussed effects as in the electron-phonon theory. For the mass enhancement, we introduce the Fermi surface (FS) average of the electronic self-energy derivative taken at the Fermi level and define

$$\lambda_{sf} = -\left\langle \frac{\partial \Sigma(\mathbf{k}, \omega)}{\partial \omega} \Big|_{\omega=0} \right\rangle_{FS} \quad (5)$$

For the Coulomb interaction operating at large energy scale, we introduce the effective parameter μ_m^* which should now refer to the same pairing symmetry m as λ_{\max} . We therefore have the effective coupling constant

$$\lambda_{eff} = \frac{\lambda_{\max} - \mu_m^*}{1 + \lambda_{sf}} \quad (6)$$

that should determine T_c .

III. RESULTS

a. Calculated Superconducting Properties in $HgBa_2CuO_4$

Here we discuss the results of our calculated superconducting properties for $HgBa_2CuO_4$ such as the en-

ergy gap function $\Delta_S(\mathbf{k}j)$ and the behavior of the maximum eigenvalue λ_{\max} describing the strength of the spin fluctuational pairing. We use the full potential linear muffin-tin orbital method [48] to calculate its LDA energy bands and wave functions. The results show a rather simple band structure near the Fermi surface composed primarily of the $d_{x^2-y^2}$ states of Cu hybridized with O_{p_x, p_y} orbitals on the square lattice as is well known from the pioneering work of Emery[49]. We then utilize the LDA+FLEX(RPA) evaluation of the pairing interaction $K_{a_1 a_2 a_3 a_4}^{(S)}(\mathbf{q})$ on the $20 \times 20 \times 4$ grid of the \mathbf{q} points in the Brillouin Zone (198 irreducible points). We use Hubbard interaction parameter U for the d-electrons of Cu as the input to this simulation, which we vary between 2.5 and 4.5 eV. We also introduce the doping by holes using the virtual crystal approximation.

The Fermi surface is triangularized onto small areas δA_i described by about 1,600 Fermi surface momenta k_i for which the matrix elements of scattering between the Cooper pairs, $M^{(S)}(\hat{k}_i, \hat{k}_{i'})$, are evaluated. The linearized BCS gap equation is then exactly diagonalized and the set of eigenstates $\lambda^{(\kappa)}, \Delta_S^{(\kappa)}(\hat{k}_i)$ is obtained for both $S = 0$ and $S = 1$ pairings. The highest eigenvalue $\lambda^{(m)} = \lambda_{\max}$ represents the physical solution and the eigenvector corresponds to superconducting energy gap function $\Delta_S^{(m)}(\mathbf{k}j)$.

The result of this simulation is that $\Delta_{S=0}^{(m)}(\mathbf{k}j)$ shows a much celebrated d-wave behavior of $x^2 - y^2$ symmetry (the lobes pointing along k_x and k_y directions) This happens for dopings $\delta \leq 0.3$ that we used in the simulation. A typical behavior of this function is shown on Fig.1(a) for $U = 4$ eV and $\delta = 0$, where the blue/red color corresponds to negative/positive values of Δ . The zeroes of the gap function are along (11) direction which are colored in grey. This result is not surprising given the strong nesting property of the Fermi surface around $(\pi, \pi, 0) 2\pi/a$ point of the Brillouin Zone as was emphasized many times in the past.

We also studied the effect of higher dopings $\delta = 0.4 - 0.5$. At those values, the gap function retains the nodal lines along (11) but develops a rather complex sign-changing behavior along the lobes by acquiring higher order harmonics. We illustrate the solution in Fig.1(b) for $\delta = 0.4$ and $U = 3.3$ eV. Such oscillatory behavior would carry an additional kinetic energy and should be less favorable energetically.

We further analyze the behavior of the highest eigenvalue λ_{\max} as a function of U and doping. The plot of λ_{\max} vs. U is shown in Fig.2 for hole dopings $\delta = 0.0, 0.1, 0.2$. In particular, one can see pretty big λ' s once we approach the spin density wave instability for U 's close to 4 eV. Unfortunately, this sensitivity imposes some challenges regarding the predictions for T_c . It is however clear that if one adopts a constant U value for all dopings, this plot will be incompatible with the well-

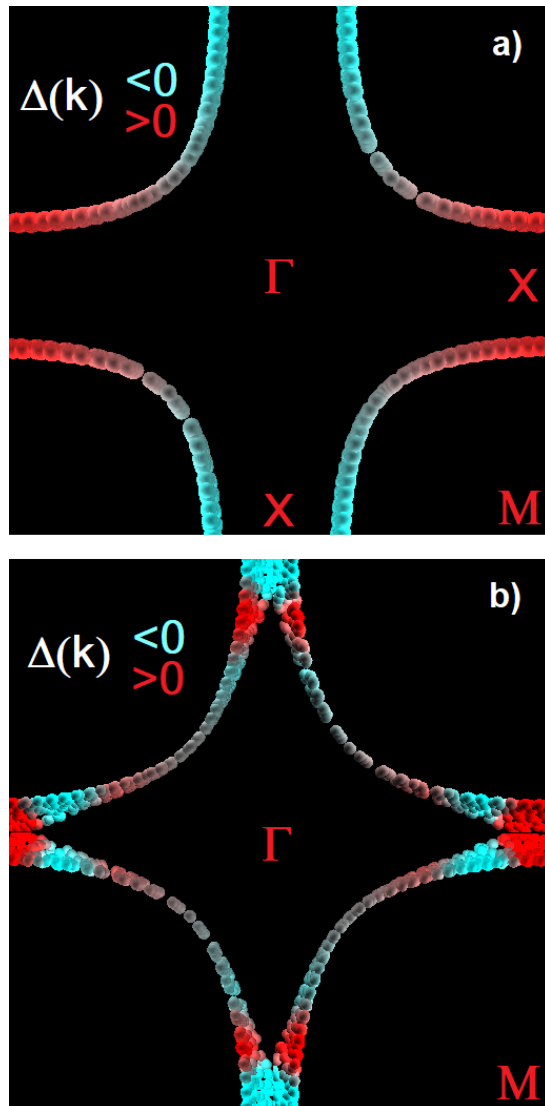


FIG. 1: Calculated superconducting energy gap $\Delta(\mathbf{k})$ for singlet pairing in $\text{HgBa}_2\text{CuO}_4$ using numerical solution of the linearized BCS gap equation with the pairing interaction evaluated using the LDA+FLEX(RPA) approach described in text. Blue/red color corresponds to the negative/positive values of $\Delta(\mathbf{k})$. Plot a) is obtained for doping $\delta = 0$ and shows typical $d_{x^2-y^2}$ behavior that is also seen for dopings $\delta \leq 0.3$. Plot b) corresponds to $\delta = 0.4$ and shows more oscillating behavior highlighting the presence of higher-order harmonics.

known dome-like behavior of the T_c vs. doping. Rather, one need to assume that for the undoped case U is largest to trigger the antiferromagnetic instability but then it gradually decreases with doping.

It is interesting to mention several works that do indeed see that U decreases with doping. A recent work[50] reported computation of doping dependent U using the constrained RPA (cRPA) procedure. Their reported values of $U \approx 4$ eV for $\text{HgBa}_2\text{CuO}_4$ are very close to the ones needed to produce large λ_{\max} , as seen in Fig. 2, together

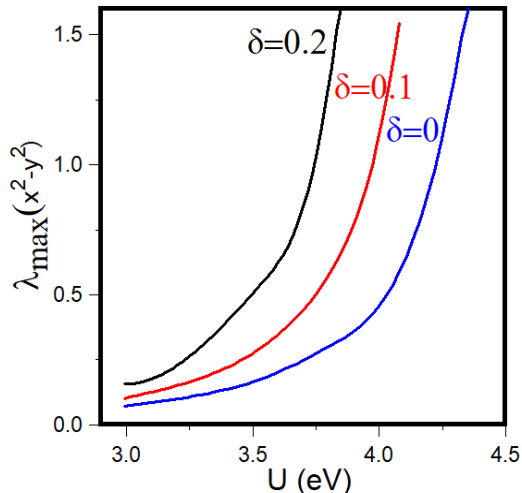


FIG. 2: Calculated dependence of maximum eigenvalue λ_{\max} of the linearized BCS equation as a function of the on-site Hubbard interaction U for d -electrons of Cu and for several hole dopings $\delta = 0, 0.1, 0.2$ in $\text{HgBa}_2\text{CuO}_4$. Large values of λ_{\max} are seen for the values of U close to the antiferromagnetic instability.

with the trend that U decreases with doping a little bit. Another recent cRPA study reported this value to be 3eV for the same compound[51] which is again within the range of what we use in our simulation. Unfortunately, the spread in these values also indicates that we cannot rely on the present state-of-the-art calculations of U .

In a different work employing DCA[52], an effective temperature dependent coupling $\bar{U}(T)$ was introduced to parametrize the DCA pairing interaction in terms of the spin susceptibility. It was extracted between 4 and 8 in the units of the nearest neighbor hopping t . The latter is known to be around 0.5 eV in the cuprates thus placing $\bar{U}(T)$ between 2 and 4 eV. $\bar{U}(T)$ has shown a significant reduction upon doping.

At the lack of the accurate determination of U , we turn to more empirical findings whether some other well-known properties of the cuprates can be reproduced using our implemented LDA+FLEX(RPA) method. Those are related to the normal state electronic structure and the extracted quasiparticle mass enhancement, $m^*/m = 1 + \lambda_{sf}$. These data are needed to determine the effective coupling constant, Eq. (6) and give estimates for the T_c . They will be discussed below.

b. Calculated Correlation Effects in Electronic Structure of $\text{HgBa}_2\text{CuO}_4$

Here we discuss our calculated properties of $\text{HgBa}_2\text{CuO}_4$ in the normal state. The self-energy

is computed by utilizing procedure described in Ref. [32] with full frequency resolved dynamical interaction matrix \hat{K} , Eq. (1). This is done as a "one-shot" calculation using the Green functions obtained from the LDA band structure, without feedback of the self-energy that will lead to "dressed" Green functions. Due to the existence of a generating functional for FLEX approximation[22], the self-consistency with respect to the Green functions can in principle be considered. There is one complication which makes such implementation not straightforward and time consuming that once complex self-energy is introduced, single-particle excitations are damped and no longer represented by the real energy bands $\epsilon_{\mathbf{k}j}$. A general formulation via, for example, imaginary Matsubara frequencies is needed. The effect of such self-consistency was studied earlier using the GW method[37] with applications to some real materials[53]. The outcome is that self-consistency worsens the agreement of the one-electron spectra with experiment. Therefore the advantage of the self-consistent implementation within perturbation theory is not obvious in general.

Nevertheless, this issue may deserve a further investigation since cuprates are doped Mott insulators in close proximity to the Mott transition and it is known that in this regime, the self-consistency is an important step when using, for example, dynamical mean field theory. Although not currently implemented by us, one can adopt a simplified version of the self-consistency with respect to quasiparticles, *i.e.*, when not the full self-energy but its value at $\omega = 0$ and its frequency derivative around $\omega = 0$ describing the quasiparticle mass enhancement are used to reconstruct new densities and resulting quasiparticle Green's functions. It was developed in connection with the GW approach, and was shown to reproduce the band gaps of semiconductors quite well [54]. A combination of the LDA and Gutzwiller's method (called LDA+G) explores a similar idea [55] where the variational Gutzwiller method is used to find those self-energy parameters. It was also implemented in a most recent combination of the GW and DMFT called QSGW+DMFT[56].

For the calculated Cu d -electron self-energy matrix $\Sigma_{a_1 a_2}(\mathbf{k}, \omega)$, we found the only significant matrix elements of this matrix exist for $d_{x^2-y^2}$ orbitals. This result is shown in Fig. 3 where the diagonal matrix elements, $\text{Re}\Sigma(\mathbf{k}, \omega)$, Fig. 3(a) and $\text{Im}\Sigma(\mathbf{k}, \omega)$, Fig. 3(b), of $\Sigma_{a_1 a_2}(\mathbf{k}, \omega)$ with $a_1 = a_2 = x^2 - y^2$ are plotted as a function of frequency for several \mathbf{k} points of the Brillouin Zone. A representative value of $U=4$ eV and $\delta = 0$ are used but general trends of this function are similar for the range of U 's and dopings that we study here. The Hartree Fock value for $\text{Re}\Sigma$ has been subtracted.

To illustrate the \mathbf{k} -dependence, the self-energy is plotted in Fig.3 along ΓM line of the Brillouin Zone (BZ) and also for the X point. At the energy scale $-6\text{eV} \leq \omega \leq 2\text{eV}$ that we use in Fig.3(a) and (b), we find the \mathbf{k} -dependence

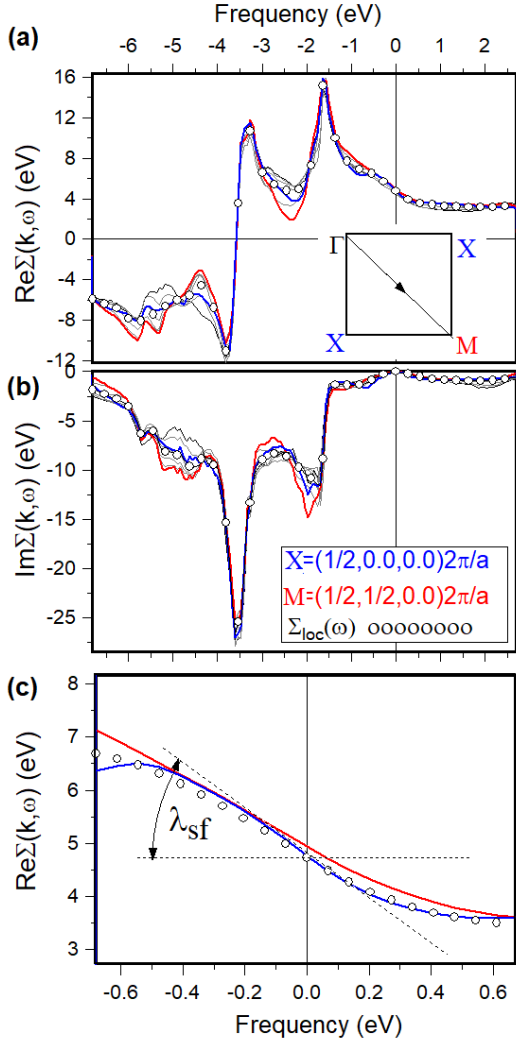


FIG. 3: Calculated $d_{x^2-y^2}$ diagonal matrix element of the self-energy $\Sigma(\mathbf{k}, \omega)$ (a is the real part, b is imaginary part, c is the real part at small energy scale) using FLEX-RPA approximation for d electrons of Cu in $\text{HgBa}_2\text{CuO}_4$. Various black curves show the self-energy for the wavevector \mathbf{k} traversing along $(\xi\xi 0)$ direction of the Brillouin Zone. Red/blue curves give the result for the M/X points of the BZ. The circles show the result of the local self-energy approximation taken as the average over all \mathbf{k} -points. A representative value of Hubbard $U=4$ eV is used and the doping δ is set to zero in this plot, but similar trends are seen for a whole range of U 's and dopings studied in this work.

to be quite small prompting that the local self-energy approximation may be adequate. This is not surprising since within RPA, $\hat{\Sigma} = \hat{G}\hat{K}$ and the range of the self-energy in real space is set by the interaction \hat{K} which describes the screening of the manifestly local U . In the \mathbf{k} space, all features in \hat{K} due to nesting come under the integral over the Brillouin Zone (BZ) and averaged out.

We subsequently evaluate numerically the local self-energy $\Sigma_{loc}(\omega)$ as an integral over all \mathbf{k} -points. Its

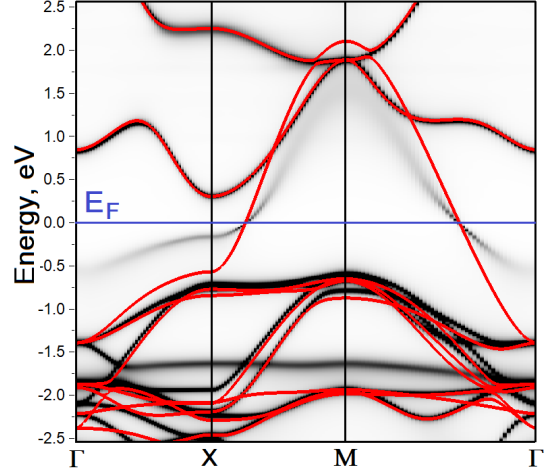


FIG. 4: Effect of the FLEX(RPA) self-energy on the calculated poles of single particle Green's functions (shown in black) for undoped $\text{HgBa}_2\text{CuO}_4$ as compared with its non-magnetic LDA band structure (red lines). The local value at $\omega = 0$ is subtracted from $\Sigma(\mathbf{k}, \omega)$ during the calculation of $\text{Im}G(\mathbf{k}, \omega)$ and the Hubbard $U=4$ eV is used.

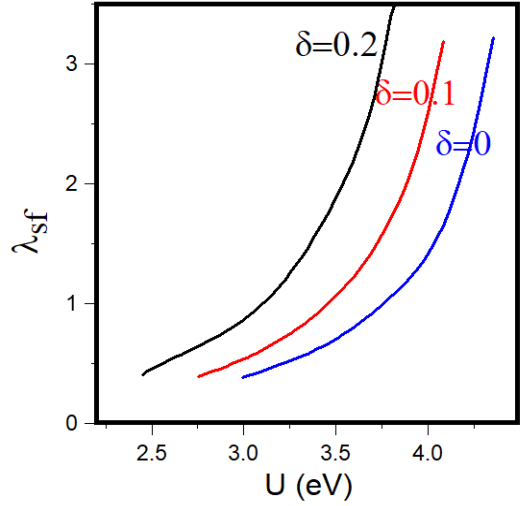


FIG. 5: Calculated dependence of the mass enhancement parameter $\lambda_{sf} = m^*/m_{LDA} - 1$ as a function of the on-site Hubbard interaction U for d-electrons of Cu and for several hole dopings $\delta = 0, 0.1, 0.2$ in $\text{HgBa}_2\text{CuO}_4$. Large values of λ_{sf} are seen for the values of U close to the antiferromagnetic instability.

frequency dependence is also shown in Fig. 3 by small circles. We see a close agreement between $\Sigma_{loc}(\omega)$ and $\Sigma(\mathbf{k}, \omega)$.

Another feature seen in this calculation is the development of pole like behavior for the self-energy at frequencies around 2 and 4 eV. Those resonances are frequently led to additional poles in the one-electron Green func-

tions that cannot be obtained using single-particle picture. The imaginary part of the self-energy is quite large which indicates the existence of strongly damped excitations. Those are usually hard to associate with actual energy bands and detect by such experimental techniques as ARPES which works best for the quasiparticles just below the Fermi energy.

Fig.3(c) shows the behavior of $\text{Re}\Sigma(\mathbf{k}, \omega)$ on the scale ± 0.6 eV with respect to the Fermi level for the two representative points M (red line) and X (blue line) of the BZ together with the momentum integrated self-energy (circles). A slight variation in the slope of the self-energy at $\omega = 0$ can be noticed as well as some differences are seen in the frequency behavior. These data are important for further analysis since the slope at $\omega = 0$ sets the mass enhancement parameter λ_{sf} for the quasiparticles as illustrated in Fig.3(c)

Based on our calculated d-electron self-energy $\Sigma(\mathbf{k}, \omega)$, we evaluate the poles of the single particle Green function. The obtained $\text{Im}G(\mathbf{k}, \omega)$ for $\text{HgBa}_2\text{CuO}_4$ is plotted in Fig. 4. Most of the poles are seen as sharp resonances (plotted in black) in the function $\text{Im}G(\mathbf{k}, \omega)$ that closely follows the energy band structure obtained by LDA plotted in red. The notable difference is seen in the behavior of the hybridized $\text{Cu}_{d_{x^2-y^2}}-\text{O}_{p_x, p_y}$ band in the vicinity of the Fermi surface that acquires a strong damping at energies away from the Fermi level. This is because our projectors allow the self-energy corrections for the Cu d-electrons only. In order to generate the $\text{Im}G(\mathbf{k}, \omega)$ we have subtracted from $\Sigma(\mathbf{k}, \omega)$ its local value $\Sigma_{loc}(\omega)$ taken at $\omega = 0$ which preserves the shape of the Fermi surface as obtained by LDA. As one sees, the primary effect of the self-energy is the renormalization of the electronic bandwidth. The mass enhancement $m^*/m_{LDA} = 1 + \lambda_{sf}$ for the Fermi electrons was found to be fairly \mathbf{k} -independent. The value of λ_{sf} was calculated numerically as the average derivative of the self-energy, Eq. (5), and estimated to be around 2.7 for $\delta = 0$ and $U = 4$ eV that we use in Fig. 4.

We further analyze the dependence of λ_{sf} on U and doping. It was found to exhibit the behavior similar to the maximum eigenvalue λ_{\max} shown in Fig.2. To generate such functional dependence we implement analytical differentiation of the self-energy at zero frequency using spectral representation for the dynamically screened interaction $K(\mathbf{q}, \omega)$ proposed many years ago[57]. Fig 5 shows the calculated behavior of λ_{sf} for dopings $\delta = 0, 0.1, 0.2$ and $2.5 \text{ eV} < U < 4.5 \text{ eV}$. Although RPA does not reproduce the metal-insulator transition, it signals its proximity via the divergence of the quasiparticle mass as the system approaches the instability.

We can compare the values of λ_{sf} with the experimentally deduced quasiparticle masses that were measured by ARPES experiments. There is some spread in this data as reported in the past literature. Doping and temperature dependence of the mass enhancement has been care-

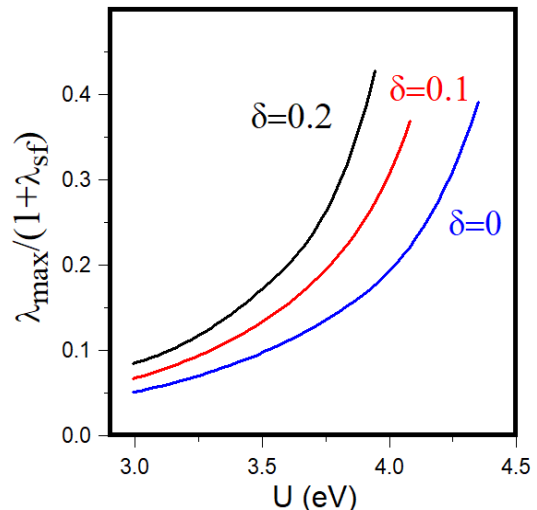


FIG. 6: Dependence of the effective spin fluctuational coupling constant λ_{eff} as a function of the on-site Hubbard interaction U for d-electrons of Cu and for several hole dopings $\delta = 0, 0.1, 0.2$ in $\text{HgBa}_2\text{CuO}_4$, calculated as the ratio between the maximum eigenvalue λ_{\max} of the gap equation and the quasiparticle mass enhancement $1 + \lambda_{sf}$.

fully studied for $\text{Bi}_2\text{Sr}_2\text{CaCu}_2\text{O}_{8+\delta}$ [58], which produced $0.5 \lesssim \lambda_{sf} \lesssim 1.7$. A later work[59] for $\text{Bi}_2\text{Sr}_2\text{CaCu}_2\text{O}_8$ and also for $\text{La}_{2-x}\text{Ba}_x\text{CuO}_4$ reported the estimate $1 \lesssim \lambda_{sf} \lesssim 2$. Somewhat larger values of the self-energy slope, $4 \div 8$, taken for several Fermi momenta have been seen in ARPES analysis of $\text{Bi}_{1.74}\text{Pb}_{0.38}\text{Sr}_{1.88}\text{CuO}_{6+\delta}$ [60]. The value of 2.7 along the nodal line was quoted for $\text{YBa}_2\text{Cu}_3\text{O}_{6.6}$ [61].

Quantum oscillations is another technique that gives the direct measure of the effective masses. The reported m^* range from 1.9 to 5 (in units of the free electron mass) for various cuprates including the value of 2.45 ± 0.15 for $\text{HgBa}_2\text{CuO}_{4+\delta}$ [62]. As the LDA band masses are not very different from the free electron masses, this indicates that $1 \lesssim \lambda_{sf} \lesssim 4$. Given the spread in these numbers, it is clear that our calculations for λ_{sf} shown in Fig 5 cover the range of the experimental data quite well.

c. Effective Coupling Constant and Estimate for T_c .

To give estimates for the effective coupling constant, λ_{eff} , Eq.(6), we first notice that for the case of angular momentum $l = 2$ relevant here, the Coulomb pseudopotential μ_m^* that projects the screened Hubbard interaction on $d_{x^2-y^2}$ cubic harmonic is expected to be very small [63]. We therefore set this parameter to zero. The plot of $\lambda_{eff} = \lambda_{\max}/(1 + \lambda_{sf})$ vs. U is shown in Fig 6 for three dopings $\delta = 0.0, 0.1, 0.2$. One can see that the range of these values is quite modest as compared to both λ_{\max} and λ_{sf} , primarily due to the fact that the

rise in the eigenvalue of the gap equation, Fig. 2, is completely compensated by the renormalization effect of the electronic self-energy, Fig. 5.

We can judge about the relevant range of λ_{eff} and deduce corresponding values of T_c using the experimentally measured mass enhancement data. Let, for example, take the middle value $\lambda_{sf} = 2$. From Fig. 5, using the values of U that produce $\lambda_{sf} = 2$, we find the corresponding values of λ_{eff} in the range $0.17 \div 0.25$ in Fig 6, depending on doping. The BCS $T_c \approx \omega_{sf} \exp(-1/\lambda_{eff}) = 1 \div 8K$ if one takes $\omega_{sf} = 40$ meV. Once we get closer to the SDW instability, the effective coupling increases to the values 0.4 as seen from Fig 6. It can go up even further by tuning U . If we consider $\lambda_{sf} = 3$, corresponding to the higher values of the mass enhancement seen experimentally, we find $0.26 \lesssim \lambda_{eff} \lesssim 0.36$ from Fig 6 and the BCS $T_c \approx 10 \div 30K$. Given the exponential sensitivity of the T_c , these estimates are certainly not far away from 100K range for which $\lambda_{eff} \approx 0.6 \div 0.7$ would be desired.

We can comment on the numerous past publications devoted to the self-consistent solution of the Eliashberg equation on imaginary Matsubara axis using RPA-FLEX and single-orbital tight-binding band structures on the square lattice. Unfortunately, due to the use of the imaginary frequencies, in most cases the theory goes straight to T_c , and it is hard to make direct comparisons to elucidate sources of possible discrepancies. In the very earlier work[6], the authors found trends very similar to ours regarding the T_c using a general $t-t'$ tight-binding model: The T_c is very small and the spin fluctuational superconductivity is strongly suppressed in the vicinity of SDW due to the renormalization effect of the electronic self-energy, while the attractive pairing was found to have a divergent character near the instability. Later solution of the same model[64] obtained $T_c = 0.02t \approx 100K$, for $U = 4t = 2eV$ and $\delta = 0.15$.

Given the last result, it is possible that our underestimation of λ_{eff} and T_c is due to the fact that we utilize the full LDA energy bands and the wave functions in the RPA-FLEX calculation. We have repeated the procedure for the single-band tight-binding model $\epsilon_k = -2t(\cos k_x a + \cos k_y a)$, and while seeing similar trends for both λ_{max} and λ_{sf} as a function of U , the evaluated λ_{eff} as the ratio $\lambda_{max}/(1 + \lambda_{sf})$ is a factor of two larger. We show the result of such calculation for $\delta = 0.1$ in Fig 7 close to the instability taking place right above $U/t = 2$. Fixing $\lambda_{sf} = 2(3)$, we extract $\lambda_{eff} = 0.62(0.78)$ and the BCS $T_c = 90K(130K)$.

A possible route for improving our approach would be to extend the BCS approximation to include full frequency dependence of the pairing interaction together with its implementation on the real frequency axis. This should allow the comparison with the BCS limit in a more controllable manner.

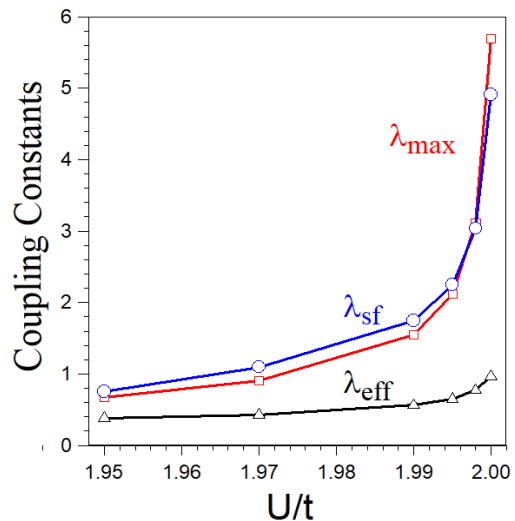


FIG. 7: Dependence of the maximum eigenvalue λ_{max} of the linearized BCS equation (red line, squares), the mass enhancement parameter λ_{sf} (blue line, circles) and the effective spin fluctuational coupling constant $\lambda_{eff} = \lambda_{max}/(1 + \lambda_{sf})$ (black line, triangles) as a function of the on-site Hubbard interaction U for the single-band Hubbard model with $\epsilon_k = -2t(\cos k_x a + \cos k_y a)$ and doping $\delta = 0.1$ solved using the RPA(FLEX) method.

IV. CONCLUSION.

In conclusion, we have implemented the electronic structure calculation of the superconducting pairing interaction using our recently developed LDA+FLEX(RPA) method that accounts for the electronic self-energy of the correlated electrons using a summation of the particle-hole bubble and ladder diagrams. Based on this procedure, the superconducting scattering matrix elements between the Cooper pairs have been evaluated numerically which served as the input to numerical diagonalization of the linearized BCS gap equation, whose maximum eigenvalue λ_{max} is seen as the superconducting coupling constant. The goal of this approach was to establish the numerical procedure to evaluate material specific λ without reliance on tight-binding approximations of the electronic structure.

A case study of the prototype cuprate superconductor $HgBa_2CuO_4$ was presented where we found a much celebrated d-wave ($x^2 - y^2$ type) symmetry of the superconducting energy gap as the favorable solution for the whole range of dopings and on-site Hubbard interactions U that were used in our simulations. A strong dependence of λ_{max} as a function of U was seen in the vicinity of antiferromagnetic instability. The same was true for the calculated quasiparticle mass enhancement $m^*/m_{LDA} = 1 + \lambda_{sf}$ in the normal state. The effective spin fluctuational coupling constant $\lambda_{eff} = \lambda_{max}/(1 + \lambda_{sf})$ was deduced, but found to be modest and incapable to deliver

high values of T_c unless U is tuned to be close to SDW. Taking the experimental constraint for $\lambda_{sf} \lesssim 3$ we have obtained the coupling constant $\lambda_{eff} \lesssim 0.4$ and the BCS $T_c \lesssim 30K$. Application of the same procedure to the 2D Hubbard model with nearest neighbor hoppings returns $\lambda_{eff} \approx 0.6 \div 0.8$ and $T_c \approx 90 \div 130K$.

At the end, we hope that with gaining further insights on other unconventional superconductors using this approach and its further improvements will ultimately allow us to reach a more quantitative understanding of unconventional superconductivity in cuprates and other systems.

-
- [1] The 1987 Nobel Prize in Physics: J. G. Bednorz and K. A. Müller for their important break-through in the discovery of superconductivity in ceramic materials.
- [2] D. J. Scalapino, E. Loh, Jr., and J. E. Hirsch, Phys. Rev. B **34**, 8190 (1986).
- [3] K. Miyake, S. Schmitt-Rink, and C. M. Varma, Phys. Rev. B **34**, 6554 (1986).
- [4] J. G. Bednorz and K. A. Müller, "Possible High T_c Superconductivity in Ba-La-Cu-O system", Z. Phys. B - Condensed Matter, **64**, 189 (1986).
- [5] For a review, see, e.g., A.V.Chubukov, D. Pines, J. Schmalian in "The Physics of Conventional and Unconventional Superconductors" edited by K.H. Bennemann and J.B. Ketterson (Springer-Verlag, 2002).
- [6] H. Shimahara, S. Takada, J. Phys. Soc. Japan **57**, 1044 (1988).
- [7] P. Monthoux, A. V. Balatsky and D. Pines, Phys. Rev. Lett **67**, 3448 (1991).
- [8] R. Arita, K. Kuroki, and H. Aoki, Phys. Rev B **60**, 141585 (1999).
- [9] T. Takimoto, T. Hotta, and K. Ueda, Phys. Rev B **69**, 104504 (2004).
- [10] I. I. Mazin and David J. Singh, Phys. Rev. Lett. **79**, 736 (1997).
- [11] T. Takimoto, Phys. Rev. B **62**, 14641 (2000).
- [12] K. Yada and H. Kontani, J. Phys. Soc. Japan **74**, 2161 (2005).
- [13] T. Ikeda, J. Phys. Soc. Japan. **77**, 123707 (2008).
- [14] J. Zhang, R. Sknepnek, and J. Schmalian, Phys. Rev. B **82**, 134527 (2010).
- [15] Zi-Jian Yao, Jian-Xin Li, and Z. D. Wang, New Journal of Physics **11**, 025009 (2009).
- [16] S. Graser, A. F. Kemper, T. A. Maier, H.-P. Cheng, P. J. Hirschfeld, and D. J. Scalapino, Phys. Rev. B **81**, 214503 (2010).
- [17] T. Takimoto, T. Hotta, and K. Ueda, J. Phys. Soc. Japan **77**, 054707 (2008)
- [18] Y. Tada , N. Kawakami, and S. Fujimoto, J. Phys. Soc. Japan **77**, 054707 (2008).
- [19] N. Kitamine , M. Ochi , and K. Kuroki, Phys. Rev. R **2**, 042032 (2020).
- [20] Y. Zhang, L.-F. Lin, A. Moreo, T. A. Maier, and E. Dagotto, arXiv:2307.15276.
- [21] For a review, see, e.g., Theory of the Inhomogeneous Electron Gas, edited by S. Lundqvist and S. H. March (Plenum, New York, 1983).
- [22] N. E. Bickers, D. J. Scalapino and S. R. White, Phys. Rev. Lett. **62**, 961 (1989).
- [23] B. Menge and E. Müller-Hartmann, Z. Phys. B: Cond. Mat. **82**, 237 (1991).
- [24] S. Doniach and S. Engelsberg, Phys. Rev. Lett. **17**, 750 (1966).
- [25] N. F. Berk and J. R. Schrieffer, Phys. Rev. Lett. **17**, 433 (1966).
- [26] For a review, see, e.g., Y. Yanase, T. Jujo, T. Nomura, H. Ikeda, T. Hotta, K. Yamada, Physics Reports **387**, 1 (2003).
- [27] A. I. Lichtenstein, M. I. Katsnelson, Phys. Rev. B **57**, 6884 (1998).
- [28] For a review, see, e.g, G. Kotliar, S. Y. Savrasov, K. Haule, V. S. Oudovenko, O. Parcollet, C.A. Marianetti, Rev. Mod. Phys. **78**, 865-951, (2006).
- [29] M. Kitatani, N. Tsuji, and H. Aoki, Phys. Rev. B **92**, 085104 (2015).
- [30] T. A. Maier, M. Jarrell, and D. J. Scalapino, Phys. Rev. B **74**, 094513 (2006).
- [31] P. Mai, G. Balduzzi, S. Johnston, and T. A. Maier, Phys. Rev. B **103**, 144514 (2021).
- [32] S. Y. Savrasov, G. Resta, X. Wan, Phys. Rev. B **97**, 155128 (2018).
- [33] V. I. Anisimov, J. Zaanen, and O. K. Andersen, Phys. Rev. B **44**, 943 (1991).
- [34] V. I. Anisimov, F Aryasetiawan and A. I. Lichtenstein, J. Phys. Condens. Mat. **9**, 767 (1997).
- [35] S. N. Putilin, E. V. Antipov, O. Chmaissem & M. Marezio, Nature **362**, 226 (1993).
- [36] In fact, both the LMTO and LAPW methods assume improved projectors that include both the radial wave functions and their energy derivatives in order to better describe orbital partial characters of the one-electron states. See, O. K. Andersen, Phys. Rev. B **12**, 3050 (1975).
- [37] For a review, see, e.g, F. Aryasetiawan, O. Gunnarsson, Rep. Prog. Phys. **61**, 237 (1998).
- [38] S. Y. Savrasov and D. Y. Savrasov, Phys. Rev. B **54**, 16487 (1996).
- [39] P. Morrel and P. W. Anderson, Phys. Rev. **125**, 1263 (1962).
- [40] W. L. McMillan, Phys. Rev. **167**, 331 (1968).
- [41] For a review, see, e.g., M. Fujita, H. Hiraka, M. Matsuda, M. Matsuura, J. M. Tranquada, S. Wakimoto, G. Xu, and K. Yamada, J. Phys. Soc. Japan **81**, 011007 (2012).
- [42] H. A. Mook, M. Yethiraj, G. Aeppli, T. E. Mason, and T. Armstrong, Phys. Rev. Lett. **70**, 3490 (1993).
- [43] For a review, see, e.g., A. Damascelli, Z. Hussain, and Z.-X. Shen, Rev. Mod. Phys. **75**, 473 (2003).
- [44] A. Lanzara, P. V. Bogdanov, X. J. Zhou, S. A. Kellar, D. L. Feng, E. D. Lu, T. Yoshida, H. Eisaki, A. Fujimori, K. Kishio, J.-I. Shimoyama, T. Noda, S. Uchida, Z. Hussain & Z.-X. Shen, Nature **412**, 510 (2001).
- [45] S. Y. Savrasov and O. K. Andersen, Phys. Rev. Lett. **77**, 4430 (1996).
- [46] F. Giustino, M. L. Cohen and S. G. Louie, Nature **452**, 975 (2008).
- [47] R. Coldea, S. M. Hayden, G. Aeppli, T. G. Perring, C. D. Frost, T. E. Mason, S. W. Cheong, and Z. Fisk, Phys. Rev. Lett. **86**, 5377 (2001).
- [48] S. Y. Savrasov, Phys. Rev. B **54**, 16470 (1996).
- [49] V.J. Emery, Phys. Rev. Lett. **58**, 2794 (1987).
- [50] J.-B. Morée , M. Hirayama, M. T. Schmid, Y. Yamaji,

- and M. Imada, Phys. Rev B **106**, 235150 (2022).
- [51] S. Teranishi, K. Nishiguchi, and K. Kusakabe, J. Phys. Soc. Japan **87**, 114701 (2018).
- [52] T. A. Maier, A. Macridin, M. Jarrell, and D. J. Scalapino, Phys. Rev. B **76**, 144516 (2007).
- [53] A. Kutepov, S. Y. Savrasov, and G. Kotliar, Phys. Rev. B **80**, 041103 (2009).
- [54] M. van Schilfgaarde, T. Kotani, S. Faleev, Phys. Rev. Lett. **96**, 226402 (2006).
- [55] X.Y. Deng, L. Wang, X. Dai, and Z. Fang, Phys. Rev. B **79**, 075114 (2009).
- [56] S. Choi, A. Kutepov, K. Haule, M. van Schilfgaarde, G. Kotliar, NPJ Quantum Materials **1**, 16001 (2016).
- [57] E. Stenzel and H. Winter, J. Phys. F: Met. Phys. **16**, 1789 (1986).
- [58] P. D. Johnson, T. Valla, A. V. Fedorov, Z. Yusof, B. O. Wells, Q. Li, A. R. Moodenbaugh, G. D. Gu, N. Koshizuka, C. Kendziora, Sha Jian, and D. G. Hinks, Phys. Rev. Lett. **87**, 177007 (2001).
- [59] T. Valla, T. E. Kidd, W.-G. Yin, G. D. Gu, P. D. Johnson, Z.-H. Pan, and A. V. Fedorov, Phys. Rev. Lett. **98**, 167003 (2007).
- [60] B. P. Xie, K. Yang, D. W. Shen, J. F. Zhao, H. W. Ou, J. Wei, S. Y. Gu, M. Arita, S. Qiao, H. Namatame, M. Taniguchi, N. Kaneko, H. Eisaki, K. D. Tsuei, C. M. Cheng, I. Vobornik, J. Fujii, G. Rossi, Z. Q. Yang, and D. L. Feng, Phys. Rev. Lett. **98**, 147001 (2007).
- [61] T. Dahm, V. Hinkov, S. V. Borisenko, A. A. Kordyuk, V. B. Zabolotnyy, J. Fink, B. Büchner, D. J. Scalapino, W. Hanke and B. Keimer, Nature Physics **5**, 217 (2009).
- [62] N. Barišić, S. Badoux, M. K. Chan, C. Dorow, W. Tabis, B. Vignolle, G. Yu, J. Béard, X. Zhao, C. Proust, M. Greven, Nature Physics **9**, 761 (2013).
- [63] A. S. Alexandrov, Phys. Rev. B **77**, 094502, (2008).
- [64] R. Arita, K. Kuroki and H. Aoki, J. Phys. Soc. Japan, **69**, 1181 (2000).